UNIVERSITY OF MINNESOTA
ST. ANTHONY FALLS LABORATORY
Engineering, Environmental and Geophysical Fluid Dynamics

Project Report No. 455

A Stochastic Imprint of Internal Physical Processes in Stratified Lake Temperatures

by

Jesús Zepeda-Arce and Heinz G. Stefan

Prepared with

Supercomputing Institute
University of Minnesota

July 2002
Minneapolis, Minnesota

UNIVERSITY OF MINNESOTA

Supercomputing Institute for Digital Simulation and Advanced Computation

Research Report

UMSI 2002/62 May 2002

Stochastic Imprint of Internal Physical Processes in Stratified Lake Temperatures

Jesús Zepeda-Arce and Heinz G. Stefan

599 Walter Library • 117 Pleasant St. SE • Minneapolis, MN 55455

1 INTRODUCTION/OBJECTIVE

One of the goals of limnology is to develop methods that can explain or predict water motion (e.g., currents and eddies), chemical processes, and biological/ecological interactions in a lake from the largest (basin) scale to the smallest (turbulence) scale. A major limitation on physical methods is the need to specify energy transfers and the dissipation at the smaller scales (e.g., internal waves and turbulent motion), furthermore to identify and to quantify the important interactions among organisms and chemicals (*Stumm*, 1985 and *Reynolds*, 1994).

The goal of this paper is inverse to physical lake process modelling. Using data from high-resolution (in time) thermistor stations in a lake, the objective is to identify different lake strata based on periodicities in the temperature signatures and to explain the stratification of the water column and its response to the wind forcing, daily heating and cooling, mesoscale and seasonal weather patterns, etc. in terms of stochastic temperature imprints. The variability of the "temperature wave spectrum" with depth season is identified and is related to the energy flux from basin-scale waves to shorter internal waves and, ultimately, to dissipation. The lake selected for study is a small lake, Lake McCarrons located in Roseville, Minnesota, at 45^o northern latitude in a temperate, continental climate.

2 DATA COLLECTED

Lake McCarrons (Figure 1), has a surface area of 0.329 km^2 and mean and maximum depths of 7.7 and 17.3 meters (25.0 and 57.0 feet), respectively. The lake is strongly dimictic and the hypolimnion becomes anoxic early in the summer and, depending on the extent of the fall turn over, may remain anoxic through the winter (*West-Mack and Stefan*, 2000). The hydrologic response of the lake is complicated by the presence of a wetland between the tributary and the lake. Wetlands are known to modify water temperatures by added

(longer) exposure of the tributary water to atmospheric heating and cooling (Andradottir and Nepf, 2000).

Water temperatures were recorded in the summers of 1999 and 2000 at 1 minute intervals at two stations, one in the littoral waters and one near the deepest point of the lake (Figure 1). At the two lake stations (rafts) thermistor chains linked to dataloggers were installed. The thermistor spacings with depth and the duration of thermistor operation are given on Figures 2 and 3.

The onset of temperature stratification was in April but only recorded in 2000. Stratification continues throughout the summer until the end of the record (October). A surface mixed layer is established by the end of April and lasts until the end of the record. In August, the surface waters begin to cool significantly, and from the end of August the surface mixed layer deepens rapidly.

Are water temperatures measured in the center of a small lake representative of the littoral water? To make that comparison, water temperatures were also recorded at a littoral station. The temperature stratification was very similar at the two sites, but the surface mixed layer depths were slightly smaller in the littoral water than in the center of the lake.

In Figure 2 water temperature variations on the order of 1 and 2^oC are apparent in the bandwidth of each thermistor trace. Only at the greatest depths (14.6 m and 17 m) are the fluctuations less than 1^oC. Near the surface (0.1 m and 1.1 m depths) one can identify a daily (periodic) heating and cooling pattern. Longer periodicities of several days duration in the near-surface records are also apparent. Fluctuations in the shallow littoral location (Figure 3) are more dynamic with daily temperature excursion up to 5^oC at times due to smaller thermal inertia of the shallow water.

3 STOCHASTIC ANALYSIS OF THE WATER TEMPERATURE RECORDS

The evaluation of lake temperature records included calculation of (a) the basic statistics (mean and standard deviation) of monthly temperature time series, (b) the autocorrelation coefficients and the plot of the monthly correlograms at the highest time lag resolution, and (c) the power spectra or periodograms for the monthly records.

3.1 Basic Statistics

To estimate their magnitude at different times of the season and at different depths, the monthly mean and the monthly standard deviations of the water temperatures were calculated for the data from the profundal and the littoral rafts. The monthly mean temperature profiles at the profundal location reveal the stratification over the summer (Figure 4). The monthly standard deviations (without trends) varied substantially from month to month and were much higher close to the water surface (Figure 4). The monthly standard deviation averaged over depth was $\pm 2.5^{o}C$ in May, in June and July it decreased to $\pm 2.0^{o}C$, and in August it reached a minimum value of $\pm 1.5^{o}C$. In September it increased to $\pm 2.5^{o}C$. Standard deviations in 1999 and 2000 were very similar (Table 1).

The mean monthly temperature profiles for the littoral raft showed a weak stratification from May through September (Figure 5). The standard deviations also varied from month to month and decreased from the water surface to the bottom of the lake (3.5 m). Standard deviations in the littoral water are given in Table 3. Depth by depth mean temperatures at the littoral site were higher than at the profundal site (Figures 4 and 5) and standard deviations were also greater (Tables 1 and 3). The differences are given in Table 2.

The seasonal lake temperature dynamics apparent in Figure 4 can be summarized as follows: (1) The epilimnion i.e., the warmest and upper most layer, was located between the surface and 2 m depth from April to August. Epilimnetic temperatures ranged from $8^{o}C$ in

May to $26°C$ in August. The epilimnion started to deepen to 4 m depth in September and 6 m depth in October. (2) The hypolimnion i.e., the coolest layer, was found below depths of 10 m for every month. The mean hypolimnetic temperatures remained around $5°C$ in 1999 and $6°C$ in 2000. (3) The metalimnion, where the seasonal thermocline is located and mean temperature gradients are greater than $1°C$ per meter of depth, was located between depths of 2 m and 10 m from May to August. The thermocline (maximum temperature gradient) occurred closest to the surface at about 3 m depth in April, descended to about 4 m in June, reached about 5 m in August, started to descend to 6 m in September and to 8 m in October as the fall turnover progressed.

3.2 Time Series Analysis

3.2.1 Methodology

The goal of the time series analysis was to discover the time structure of the signals measured and to describe the deterministic and stochastic components of the signal, assuming that the temperature time series were realizations of a stochastic process with a deterministic and a random component.

An important part of the time series analysis is to find the deterministic period components (*Nesmerak and Straskraba*, 1985) described by equation (1)

$$x(t) = A + \sum_{j=1}^{k} B_j \cdot \cos\left(\frac{2\pi}{T_j - \nu_j}\right) + y(t) \tag{1}$$

with $x(t)$ = value of the time series at time t, A = the average value of the time series, B_j = the amplitude of the j-th component, T_j = period of the j-th component, ν_j = the phase shift of the $j-th$ component, $y(t)$ = residual value at time t ($t = 1, 2, ..., N$). Periods, participating significantly in the periodic deterministic component can be determined by means of the autocorrelation function, periodogram or power spectrum.

The autocorrelation function $R_x(\tau)$ is given by

$$R_x(\tau) = cov[x(t), x(t+\tau)]/var[x(t)] \tag{2}$$

Equation (2) represents the ratio of the ensemble covariance to the variance of the sample time series. A plot of the autocorrelation function against the lag τ, called correlogram, is useful in determining if successive observations are independent or not.

The autocorrelation function $R_x(\tau)$ is one instrument for identification of high frequency periodicities participating in the periodic component. Another method for calculating important periods at the highest time resolution level is the power spectrum or periodogram (*Wilks*, 1995). The spectrum analysis considers that the fluctuations or variations in a time series have arisen by adding together of a series of sine and cosine functions. These trigonometric functions are "harmonic" in the sense that they are chosen to have frequencies exhibiting integer multiples of the "fundamental" frequency determined by the sample size of the data series.

The equation

$$y_t = \overline{y} + \sum_{k=1}^{n/2} \left\{ A_k \cos\left[\frac{2\pi kt}{n}\right] + B_k \sin\left[\frac{2\pi kt}{n}\right] \right\} \tag{3}$$

says that a data series y_t of length n can be completely specified by $\frac{n}{2}$ harmonic functions. The data series y_t yields a set of quantities A_k and B_k according to the following equation

$$\begin{aligned} A_k &= \frac{2}{n}\sum_{t=1}^{n} y_t \cos\left(\frac{2\pi kt}{n}\right) \\ \textit{and} & \\ B_k &= \frac{2}{n}\sum_{t=1}^{n} y_t \sin\left(\frac{2\pi kt}{n}\right) \end{aligned} \tag{4}$$

Equation (4) is called the *discrete Fourier transform.* The transform suggests that a time series consisting of a collection of data points y_t measured as function of time can be replaced by a collection of *Fourier* coefficients A_k and B_k that are a function of frequency w_k.

This new perspective allows one to see the contributions to a time series that are made by separate processes of different speeds, that is, by processes operating at a spectrum of different frequencies. *Panofsky and Brier* (1958) illustrate this distinction with a nice analogy: "An optical spectrum shows the contributions of different wave lengths or frequencies to the energy of a given light source. The spectrum of a time series shows the contributions of oscillations with various frequencies to the variance of a time series". Even if the underlying physical basis for a data series y_k is not really well represented by a series of cosines waves, much can still be learned about the data given by viewing it from this perspective.

3.2.2 Autocorrelation Results

An autocorrelation analysis was first conducted on the temperature records divided into monthly periods. Any trends in the temperature record were removed and an unbiased time series was analyzed. The following results were found from the data collected at the profundal location.

1. Correlograms for water temperature records from different depths could be lumped into four groups/types as a function of depth. The four groups/types are shown in Figures 6, 7, 8, and 9, respectively. Each group of autocorrelation coefficients showed a particular set of characteristics of the water temperature dynamics.

2. Diurnal (24-hour) temperature oscillations were found in records from water depths of 0.1 to 2.0 m in the center of the lake (Figure 6). The autocorrelation function has a daily periodicity clearly visible in Figure 6 for July and August, but also present in May and June.

3. A low frequency oscillation was found at depths from 0.1 m to 2.0 m in June. In June the oscillation had a period of about 15 days (Figure 6) in both years. In July of 1999 the period was 10 days and in May of 2000 a period of 15 days was present.

4. In the metalinion, typically between 2 m and 6 m, the correlograms lose the diurnal oscillations; the periodic component becomes weaker for temperature records from greater depths (Figure 7).

5. In the hypolimnion, i.e. at depths greater than 6 m, the temperature records showed a purely random behavior without any periodic deterministic component (Figure 8).

6. In the benthic layer at the bottom of the lake the autocorrelation coefficients (Figure 9) showed again a pronounced periodicity, and the random components were much weaker.

7. It is important to point out that from May to October of both years the autocorrelation coefficients for the hypolimnion layer were much lower and closer to zero, thus representing a purely random process as opposed to the other three layers where the periodic (deterministic) process was a key component in the temperature fluctuations.

8. For March and April of 2000 the correlograms did not show any significance difference among the four characteristic layers, indicating that the temperature dynamics at all depths were the same during the spring season, i.e. before the onset of stratification.

9. May, June, July, and August of 1999 and 2000 were the months that the autocorrelation coefficients showed diverse values among the characteristic layers.

10. In general the results for 1999 and 2000 are almost the same, although the correlograms showed a longer summer period in 2000. Because spring started earlier in 2000 (ice out was in March instead of April) a low-frequency oscillation was detected in the correlogram in May of 2000, but not until June of 1999.

Analysis of the data from the littoral (shallow) water gave the following results:

1. Three layers were detected in the patterns of the correlograms. Diurnal oscillations

were shown by the autocorrelation analysis predominantly for water depths up to 0.8 m in July and August (Figure 10).

2. Two low frequency oscillations were found for the months of June, July, and August. The oscillation had again a periodicity of 15 days in June and 10 days in July.

3. In the second layer, called "temperature gradient layer", diurnal (24-hour) oscillations disappeared but the low-frequency oscillations of June and July were still detected.

4. In the benthic layer the correlograms showed a low periodic influence compared to the two top layers that had a direct influence from the atmospheric factors a strong random behavior was detected (Figure 11).

5. Overall, the correlograms showed very similar behavior for both the littoral and the profundal water temperature records. The diurnal (24-hours) component seemed stronger and visible over a longer period in the correlogram for the littoral record, when compared to the profundal record.

3.2.3 Power Spectrum Results

Spectra were calculated for all depths and all months with records. All results are contained in a report (*Zepeda-Arce and Stefan*, 2002). In spring there was no significant difference among spectra for different depths (Figure 12) although some changes began to appear in April, especially near the lake bottom. Beginning with May, i.e. after a stratification had developed, spectra were found to be similar in the four basic layers of the lake identified earlier by standard deviations of water temperature fluctuations: surface mixed layer, metalimnion layer, hypolimnion layer and benthic layer. This is also in agreement with previous plots of the autocorrelation coefficients. However, the depths over which power spectral characteristics were similar, shifted (increased or decreased) as the season progressed. Figure 13 gives

the thicknesses of the four layers over time. To illustrate power spectral characteristics in the four layers over time, sample spectra are presented for depths of 0.1 m (surface mixed layer), 6.1 m (metalimnion), 11.1 m (hypolimnion), and 17.0 m (benthic layer). The evolution in time is given in increments of two months from May to October 1999 in Figures 14 to 16. At the profundal raft, the following characteristics were found layer by layer and month by month.

1. Surface Mixed Layer. The power spectra of this layer were fairly similar in each month from May to October. The depths over which power spectral characteristics were similar increased or decreased as the season progressed (Figure 13). Beginning with a period of 1 week, the energy decreased almost linearly and two strong oscillations were present in almost all months: a diurnal and a semidiurnal cycle. The surface mixed layer is always in contact with the atmosphere, thus its main sources of energy are solar radiation and wind. The surface mixed layer had almost 3.5 m of depth in May, then it was reduced to a depth of 2.5 m for the months of June and July. Deepening was detected in the late summer from 3.5 m (August) to 4.5 m (September), and 6.5 m (October) (Figure 13).

2. Metalimnion Layer. This layer is located below the surface mixed layer and shows high variations of energy at periods shorter than 24 hrs. The diurnal and semidiurnal oscillations have disappeared in this layer, and instead effects of internal wave oscillation are displayed. The spectra showed a rapid decrease in energy from the period of 1 month to 1 day. Then the spectrum displays a buildup of energy between the 1 day(24-hrs) period and the 1 hr period. The strong oscillation with periods near 2 hrs are produced by internal waves. Beyond the peak of this internal wave action the energy spectrum decreases linearly with the value of ω^{-1}, where ω is frequency (Imberger, 1994).

   In May the metalimnion was located between depths of 3.5 m and 5.5 m. In the warmer

months of June and July the layer started to occupy depths of 2.5 m to 10.5 m (8 m thickness). In August the water temperature decreased and the upper boundary of the metalimnion shifted to a depth of 3.5 m. By the end of the summer (September and October) the metalimnion had moved to greater depths and its thickness was reduced to about 2 m (Figure 13).

3. Hypolimnion Layer. The hypolimnion layer showed energy spectra with the following characteristics (see Figures 14 to 16): (1) a rapid loss of energy from periods of one month to one day; (2) a buildup of energy, as in the metalimnion, in the range of hourly periods, but no strong internal wave periodicity; (3) down to a period of 20 minutes a linear decrease of energy. Motion with periods of minutes are due to turbulence. The thickness of the hypolimnion layer decreased from 8.5 m in May to 4 m in June and July, then increased to a depth of 5.5 m in August and October, with a further increase to 7.5 m in September (Figure 13).

4. Benthic Layer. Near the bottom of the lake the power spectra shows two types of energy structure: the fist one for periods of 1 month to 10-12 hrs exhibits strong wave oscillation; the second is for periods between 10 hrs and 20 min the energy line is almost horizontal and motion is due to turbulence.

The same spectral analysis was applied to the data from the littoral zone of Lake McCarrons. Monthly data were analyzed for the months of May to September. Similarity in the spectra led again to the identification of three layers: A surface mixed layer, a subsurface layer and a metalimnion layer. The surface mixed layer with a constant depth of 1.8 m is somewhat thinner than at the center of the lake. The subsurface layer covers the rest of the depth down to 3.1 m except in June and July when a layer with metalimnetic characteristics develops near the bottom. Typical spectra for water temperatures at depths of 0.1 m, 2.1 m and 3.0 m are given in Figure 17.

The spectrum for the subsurface layer shows a linear drop of energy from the 1-month period to a period near 1 hr, except for a diurnal (24-hour) oscillation that it is due to the radiation penetration and convective night time turnover.

For the months of June and July (1999) the littoral power spectra displayed a benthic layer that is different from the profundal zone; it shows a fast decay of energy between the periods of 1 month and 1 week. After the 1 week period no diurnal or semidiurnal oscillations are detected, but some oscillations are shown with less than 4 hrs period and more than 0.74 hrs.

4 RELATIONSHIPS BETWEEN STOCHASTIC IMPRINTS IN WATER TEMPERATURES AND PHYSICAL PROCESSES

The results of the stochastic analysis in the foregoing section have shown several distinct periodicities in the water temperature time series. Some of the low frequencies that have become apparent in the analysis can be related to specific physical processes.

It was intriguing to find low frequency periods on the order of 10 to 15 days in the autocorrelograms for May and July (Figures 6 and 10). To shed more light on the cause of these periodicities, an analysis of the wind velocity and air temperature records over the same period was made. Wind velocity records were available from an anemometer installed at 2 m elevation on the raft in Lake McCarrons with a sampling frequency of 10 minutes. An autocorrelation analysis was performed, and as expected, the correlograms showed that the wind velocity records have only random components without any periodicity.

Daily air temperatures were also available (from the Minneapolis/St. Paul International Airport) and subjected to autocorrelation analysis. As shown in Figure 18 the air temperature series displays two periodicities, one with a period of 14 to 15 days for the month of June in 1999 and one with a period of 10 days in July 1999. Similarly a period of 15 days

in May 2000 and a period of 12 days in June 2000 were identified. These periodicities agree with those of the water temperatures in the profundal and littoral zones of Lake McCarrons, and thus provide statistical evidence that the mesoscale weather patterns produce a response in the hydrothermal behavior of a lake. Cyclic massive warm air flow from the Gulf of Mexico followed by cooler air from Canada is the likely origin of these periodic mesoscale phenomenon.

The surface mixed layer spectra show diurnal and semidiurnal oscillations as the energy decreases linearly from the 1-month period to 20-minutes. The semidiurnal oscillation may be related to the land-lake breeze in the mornings and in the evenings, due to a gradient of air temperature between the land and the lake.

Periodic diurnal water temperature variations near the surface (0 to 1.5 m) are clearly attributable to daytime heating and nighttime cooling. According to the autocorreltion analysis diurnal amplitudes vary significantly with month and depth. This can be attributed to seasonal variation of incident solar radiation and radiation attenuation with depth as well as seasonal variations in evaporative heat fluxes.

From 2 to 6 m depth, i.e. in the metalimnion, the temperature periodicities are attributable to internal waves and/or intrusions that are difficult to depict with the autocorrelation analysis due to the time-scale limitation.

For comparison with the results from the energy spectra, the period of an internal seiche based on a rectangular basin using the largest and smallest fetch of Lake McCarrons was calculated. The period of an internal uninodal seiche in a rectangular two-layered basin is given as (*Horne*, 1994)

$$T = 2L[(g(\rho_h - \rho_e)/\rho_h)/(1/z_h + 1/z_e)]^{-1/2} \tag{5}$$

where ρ_h and ρ_e are the densities of hypolimnion and epilimnion respectively, z_h and z_e are the respective thicknesses of epilimnion and hypolimnion, and L is the basin length. Lake McCarrons has a maximum length of 776 m and a maximum width of 339 m. For the

calculation of the internal seiche periods it was decided to use layer thicknesses and densities derived from the monthly mean temperature profiles at the profundal raft (see Figure 4). Internal seiche periods were calculated for the months of May, June, July, August, September, and October with the maximum and minimum fetch of Lake McCarrons (Figure 19). The dominant periods given by the power spectra are between the largest and smallest predicted values that were computed from the two-layer rectangular basin model, and are therefore interpreted as the periods of internal waves.

Below 6 m, i.e. in the hypolimnion, the temperature values become more independent from each other and a lack of periodic components is detected in the correlograms. This is evidence of turbulence, essentially a random process. At the bottom of the lake, the benthic boundary layer is characterized by the slow decay in correlation in the temperature records. The movement of water in this layer is due to internal seiche motion, internal wave reflection and breaking.

5 CONCLUSIONS

Based on measured water temperature profiles it is customary to divide stratified, dimictic lakes into three layers in which water quality differs significantly: epilimnion, metalimnion, and hypolimnion. The boundaries are usually drawn somewhat arbitrarily, based on the vertical gradients of observed/measured profiles of water temperature or other water quality parameters. Measurements are often made at weekly or bi-weekly intervals, and seasonal changes are assessed following the profiles observed at those intervals.

A complementary approach, is proposed and illustrated in this paper. It uses stochastic analysis of time series measurements in a lake. Water temperature data are used in the example, but as reliable sensors and digital data acquisition for lake water quality measurements become commercially available, time series data of other water quality parameters

will become more accessible and may be used as well.

Time series data, consist of frequent measurements of the same parameter at the same location. If records are obtained at many locations at the same time, the spatial and temporal characteristics of the water quality "domain" can be analyzed. In our example a water temperature data set obtained with two thermistorchains of 12 and 9 thermistors each, respectively, in a small but relatively deep lake was used. Data were collected every minute over 5 and 7 months in 1999 and 2000, respectively. All measurements ended in October.

The stochastic analysis of the data gave monthly mean and associate standard deviations, autocorrelation coefficients and power spectra. The interpretation of the results allows the following conclusions:

1. Using a monthly timescale it is possible to depict the seasonal variation in temperature structure and the strength of the stratification at each depth.

2. Fluctuations (standard deviations) of water temperatures around monthly mean values (trend removed) give an idea of the magnitude of variability in time, and how "representative" a single instantaneous measurement of a temperature profile may be.

3. The similarity of water temperature correlograms and spectra for different depths of a lake lead to the identification of a four layer structure: a surface mixed layer, the metalimnion, the hypolimnion, and the benthic layer. In each of the four layers the characteristics or signatures of the autocorrelograms and spectra are identical and thus suggest dynamic behavior.

4. Thicknesses and depths of the top three layers derived from stochastic similarity closely agree with those derived by the conventional approach using vertical temperature gradients.

5. Dominant frequencies found in the timeseries analysis can be linked to specific hydrodynamic and heat exchange processes and interactions with the atmosphere: mesoscale

weather systems, diurnal heating and cooling, internal waves, and boundary layer turbulence.

6. Application of stochastic tools to the time series data gives a non-deterministic perspective on how meteorological variables influence a lake at different time-scales and depths.

In this study, only one lake was analyzed. More lakes need to be analyzed in a similar way so that conclusions can be generalized. Also, for each lake, stochastic characteristics need to be linked to bathymetry and weather more directly.

6 ACKNOWLEDGMENTS

The material presented in this paper is based upon data collected by Karen Jensen and Gary Oberts of the Metropolitan Council, Environmental Services, St. Paul MN with guidance by Christopher Ellis of the University of Minnesota, St. Anthony Falls Laboratory. The first author wishes to acknowledge the support of a Fellowship by the National University of Mexico. The authors are thankful to Dr. Omid Mosheni for his suggestions on the water temperature data processing. Statistical analyses were performed at the Minnesota Supercomputer Institute (MSI), University of Minnesota.

References

[1] Andradottir, H. O., and H. M. Nepf. 2000. Thermal mediation by littoral wetlands and impact on lake intrusion depths. Water Resour. Res. 36(3): 725-736.

[2] Horne, A. J., and C. Goldman. 1994. Limnology, 576 pp. 2nd ed. McGraw-Hill. New York.

[3] Imberger, J. 1994. Transport processes in lakes: a review, p. 99-193. *In* R. Margalef [ed], Limnology now: a paradigm of planetary problems. Elsevier. Amsterdam, The Netherlands.

[4] Nesmerak, I., and M. Straskraba. 1985. Spectral analysis of the automatically recorded data from Slapy Reservoir, Czechoslovakia. Int. Revenue Ges. Hydrobiol. 70(1): 27-46.

[5] Panofsky, H. A., and G. W. Brier. 1958. Some applications of statistics to meteorology, 224 pp. University Park. Penn. State Univ.

[6] Reynolds, C. S. 1994. The role of fluid motion in the dynamics of phytoplankton in lakes and rivers, p. 141-187. *In* P. S. Giller, A. G. Hildrew, and D. G. Raffaelli [eds], 34th Symp. of the British Ecological Society, Scales, Pattern and Process. Aquatic Ecology. United Kingdom.

[7] Stumm, W. 1985. Chemical processes in lakes, 435 pp. Wiley & Sons. New York.

[8] Wilks, D. 1995. Statistical methods in the atmospheric sciences, 341 pp. Academic. San Diego, Çalif.

[9] West-Mack, D., and H. G. Stefan. 2000. Inflow dynamics and potential water quality improvement in Lake McCarrons. Proj. Rep. 448. St. Anthony Falls Lab. Univ. of Minnesota.

[10] Zepeda-Arce, J., and H. G. Stefan. 2002. Stochastic imprint in lake temperature stratification. Proj. Rep. 455. St. Anthony Falls Lab. Univ. of Minnesota.

List of Tables

Table 1: Standard deviations of monthly water temperature records at the profundal location.

		Month							
Depth (m)	Year	March	April	May	June	July	August	September	October
0.1	1999			2.44	1.76	1.77	1.33	2.36	1.64
	2000	1.29	2.47	1.97	1.89	1.59	1.35	2.26	1.50
1.1	1999			2.03	1.72	1.69	1.15	2.36	1.63
	2000	1.143	2.45	1.95	1.88	1.51	1.33	2.26	1.49
2.0	1999			1.27	1.55	1.53	0.96	2.47	1.58
	2000	0.90	2.31	1.70	1.77	1.31	1.25	2.34	1.50
3.0	1999			1.59	1.25	1.17	0.93	2.31	1.51
	2000	0.75	1.56	1.23	1.56	0.56	0.91	2.28	1.50
4.0	1999			2.52	0.77	1.01	0.36	2.14	1.41
	2000	0.66	0.74	1.74	1.17	0.86	0.83	2.20	1.53
5.1	1999			1.81	0.40	0.73	1.05	1.49	1.35
	2000	0.60	0.39	1.23	0.61	0.56	1.12	1.51	1.47
6.1	1999			0.48	0.42	0.48	0.44	1.11	1.29
	2000	0.57	0.34	0.46	0.42	0.39	0.60	0.93	1.20
7.1	1999			0.11	0.29	0.34	0.30	0.78	1.05
	2000	0.56	0.37	0.18	0.27	0.23	0.33	0.44	0.32
9.1	1999			0.19	0.23	0.25	0.21	0.20	0.20
	2000	0.57	0.44	0.05	0.09	0.10	0.13	0.13	0.18
11.1	1999			0.22	0.18	0.15	0.11	0.11	0.11
	2000	0.62	0.48	0.03	0.04	0.05	0.07	0.07	0.08
14.6	1999			0.14	0.11	0.08	0.04	0.06	0.03
	2000	0.64	0.50	0.04	0.03	0.03	0.03	0.03	0.03
17.0	1999			0.11	0.11	0.10	0.04	0.05	0.02
	2000	0.36	0.44	0.02	0.01	0.01	0.01	0.02	0.02

Table 2: Standard deviations of monthly temperature records in the littoral location.

		Month				
Depth (m)	Mean	May	June	July	August	September
0.1	1999	2.57	1.92	1.92	1.55	2.56
0.3	1999	2.53	1.90	1.89	1.52	2.55
0.6	1999	2.43	1.89	1.86	1.46	2.54
0.8	1999	2.27	1.87	1.83	1.39	2.52
1.6	1999	1.35	1.80	1.67	1.26	2.42
2.1	1999	1.01	1.57	1.47	1.23	2.34
2.6	1999	0.99	1.33	1.30	1.20	2.24
3.0	1999	1.14	1.28	1.28	1.05	2.29
3.1	1999	1.24	1.28	1.28	0.97	2.32

Table 3: Mean monthly water temperature differences between the profundal site and the littoral site (1999).

	Month $\overline{T}_{prof} - \overline{T}_{litt}$				
Depth (m)	May	June	July	August	September
0.1	0.04	0.04	-0.09	-0.32	-1.72
1.1/0.8	-0.08	0.11	0.02	-0.24	-1.64
2.0/2.1	0.07	0.35	0.35	0.08	-1.34
3.0	-0.37	0.31	0.61	-0.25	-1.38

List of Figures

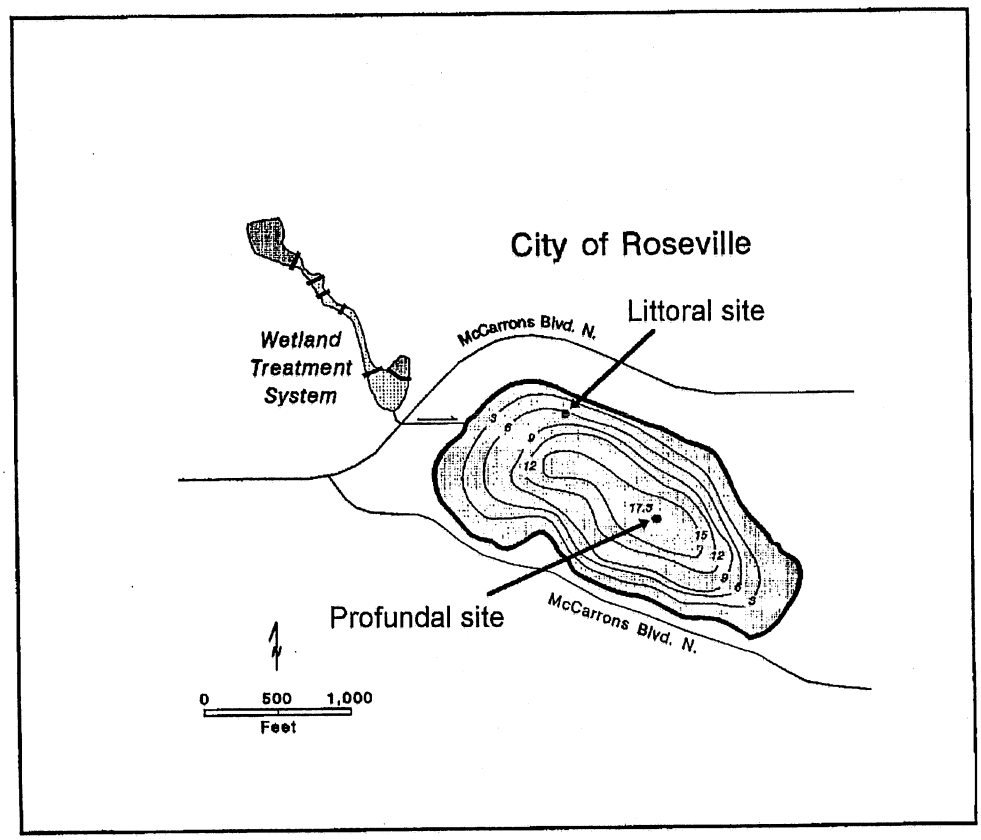

Figure 1: Lake McCarrons Bathymetry and Location.

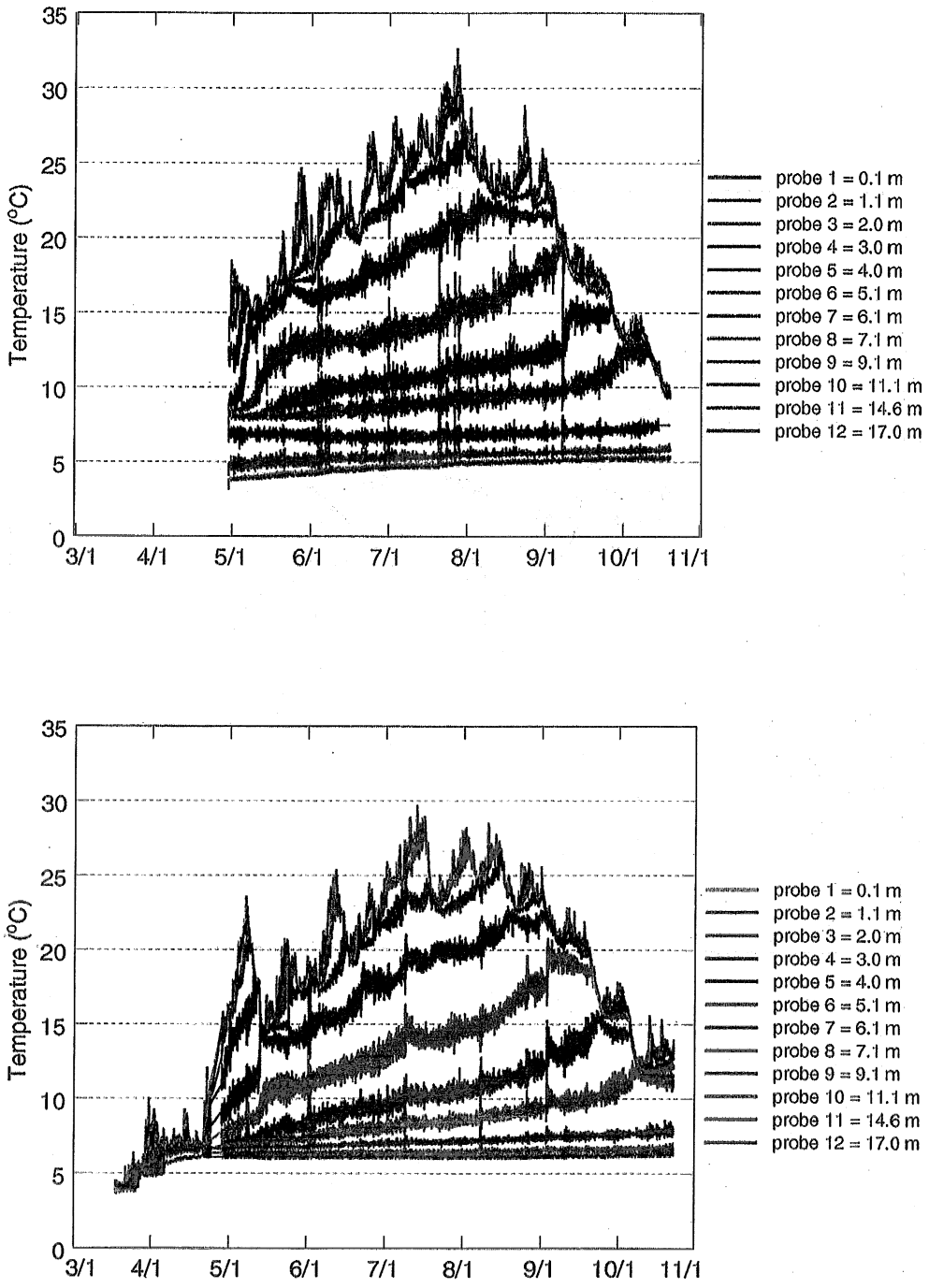

Figure 2: Water temperature time series at different depths in the center region region of Lake McCarrons, in 1999 (top) and 2000 (bottom). The highest and lowest water temperatures are for probe 1 and probe 12, respectively.

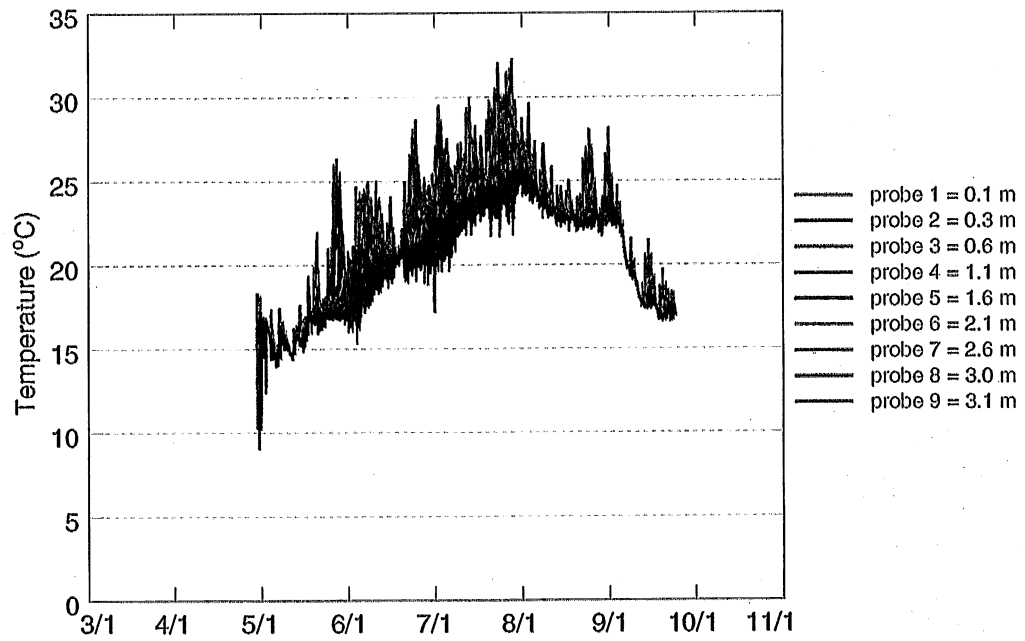

Figure 3: Water temperature time series at different depths in the littoral region of Lake McCarrons, 1999. The highest and lowest water temperatures are for probe 1 and probe 9, respectively.

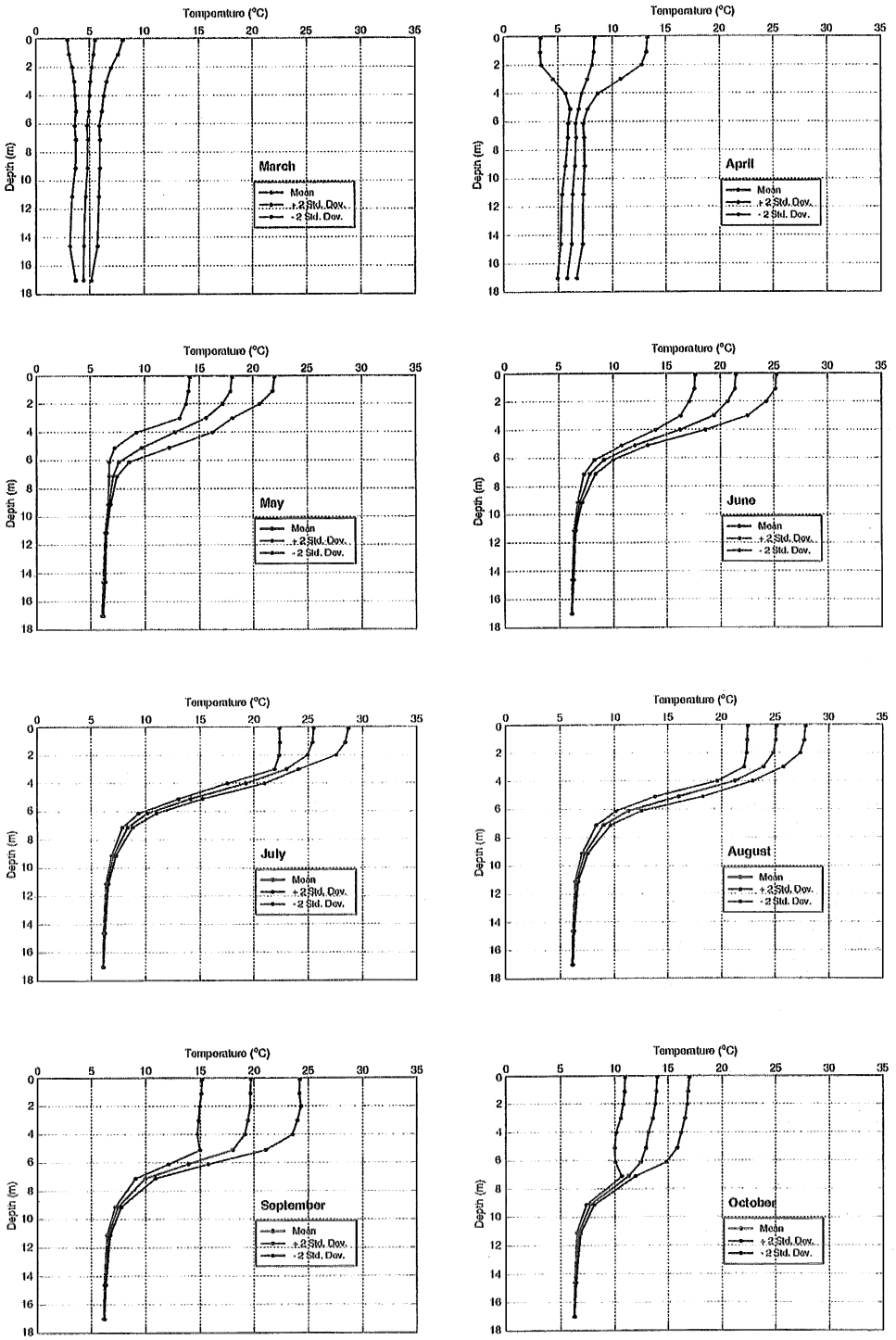

Figure 4: Monthly average and standard deviation of 10-min average water temperatures in McCarrons Lake from March to October 2000.

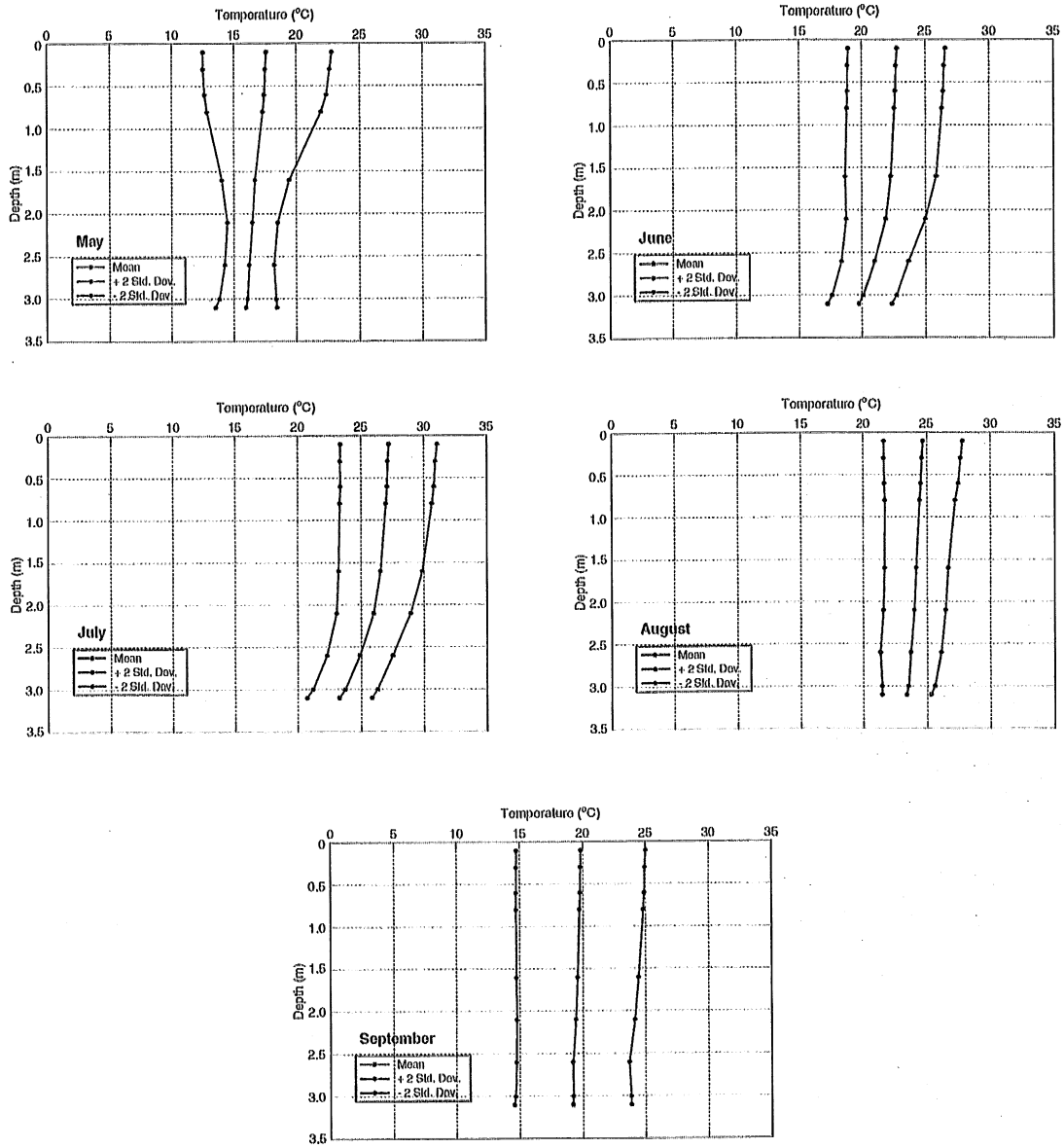

Figure 5: Monthly average and standard deviation of the 10-min average water temperatures of McCarrons Lake from May to September 1999.

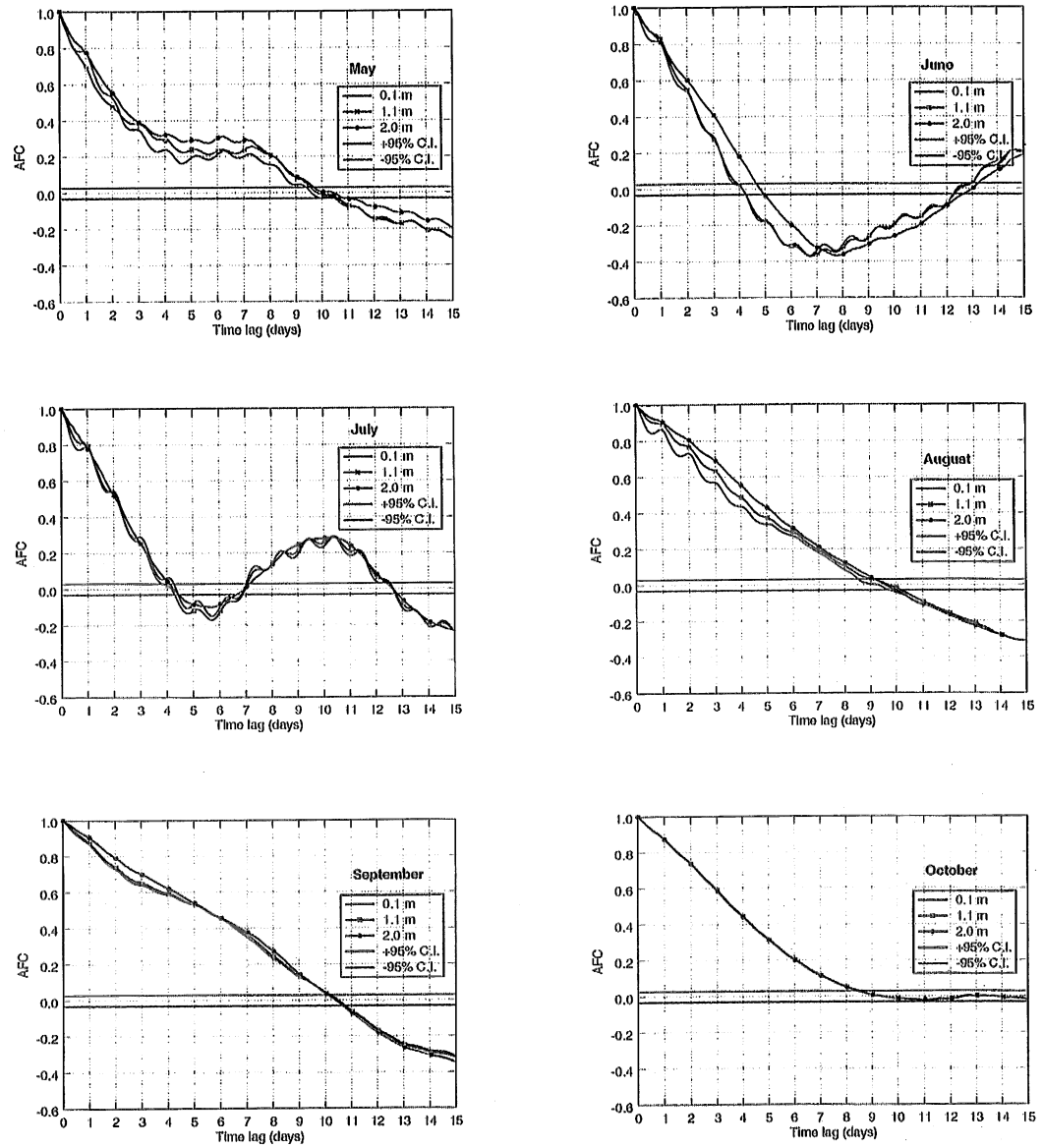

Figure 6: Autocorrelation coeffients of the temperature records for the surface mixed layer (depths of 0.1, 1.1, and 2.0 m) in the center of Lake McCarrons for the months of May to October 1999.

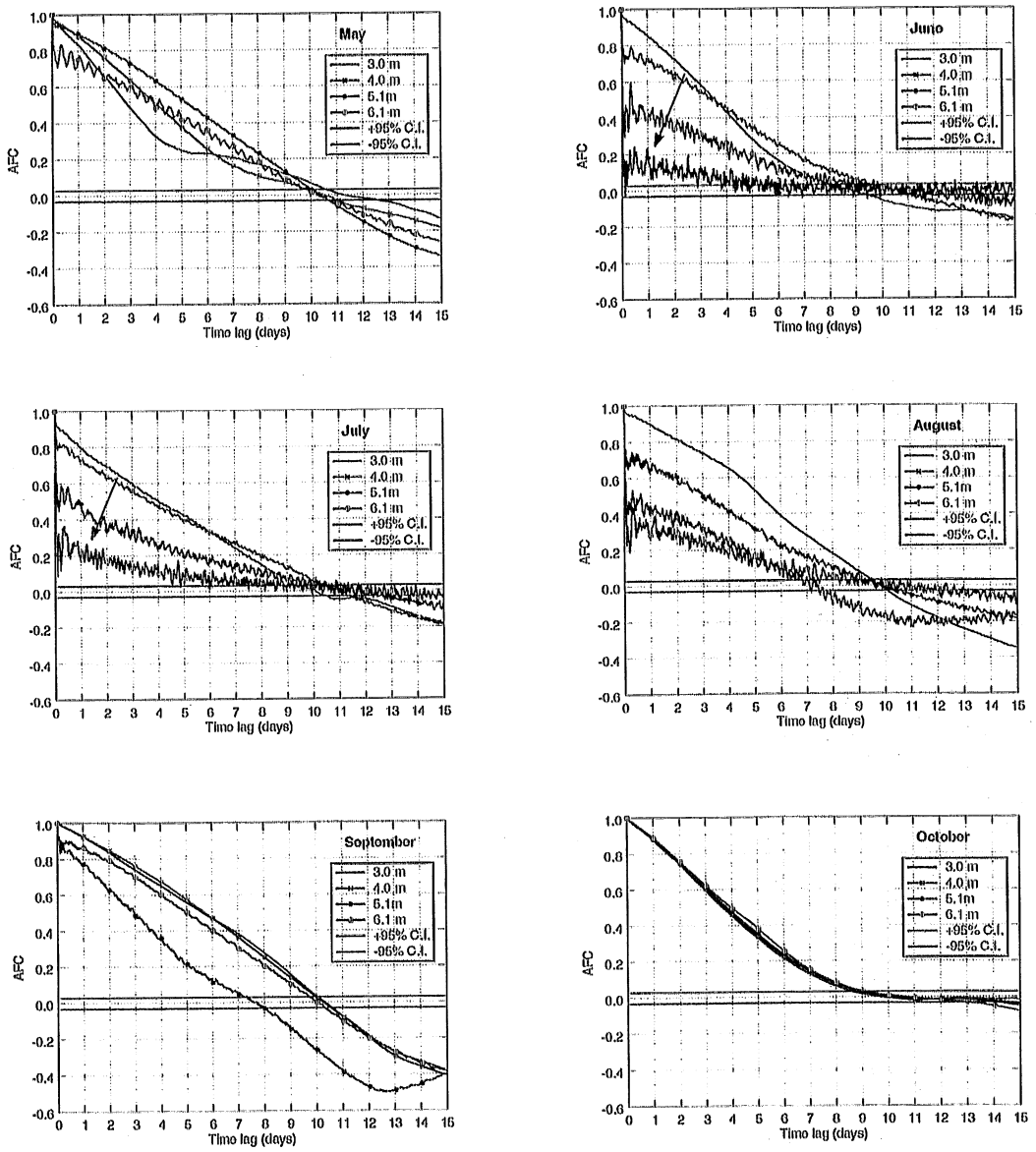

Figure 7: Autocorrelation coeffients of the temperature records for the metalimnetic layer (depths of 3.0, 4.0, 5.1, and 6.1 m) in the center of Lake McCarrons for the months of May to October, 1999.

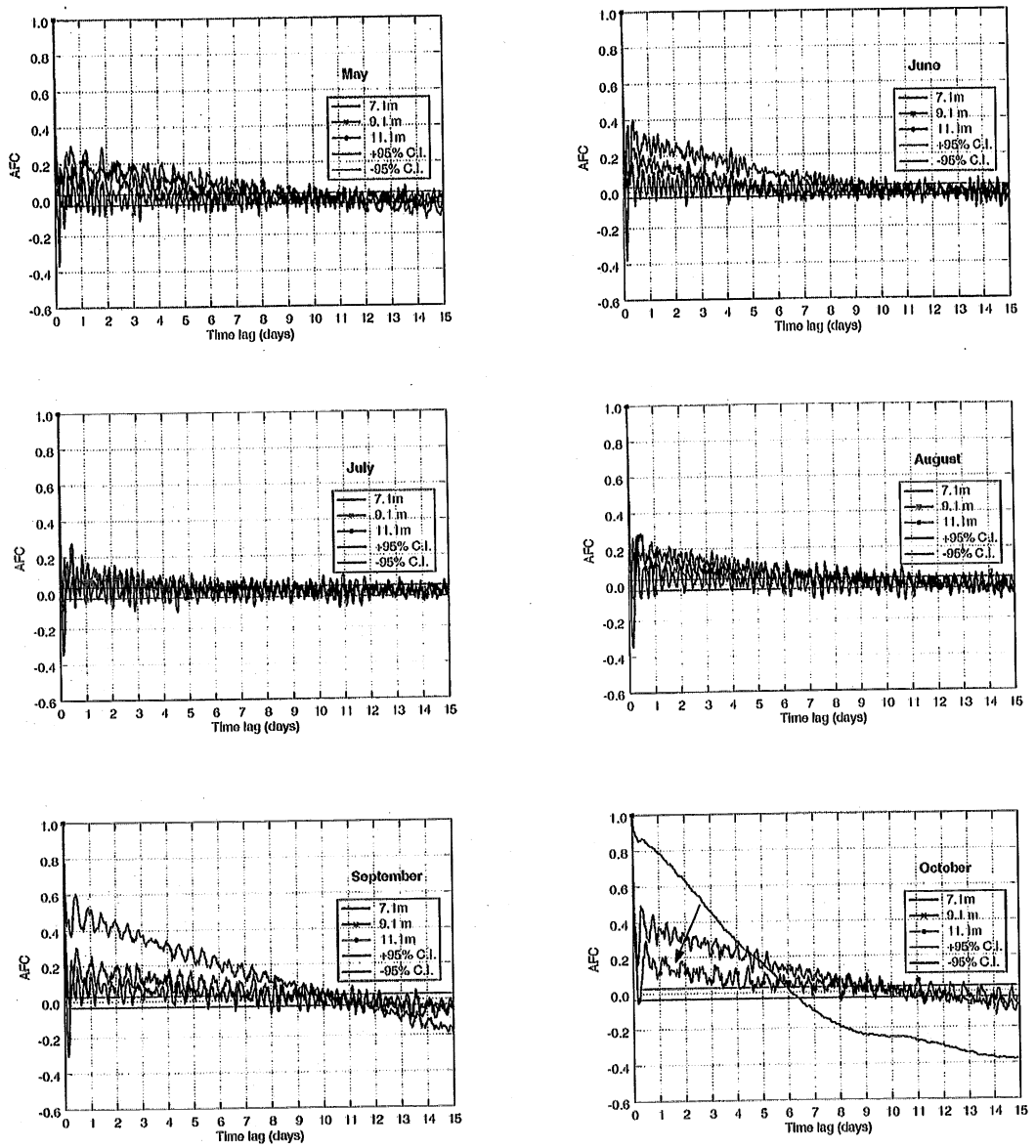

Figure 8: Autocorrelation coeffients of the temperature records for the hypolimnetic layer (depths of 7.1, 9.1, and 11.1 m) in the center of Lake McCarrons for the months of May to October, 1999.

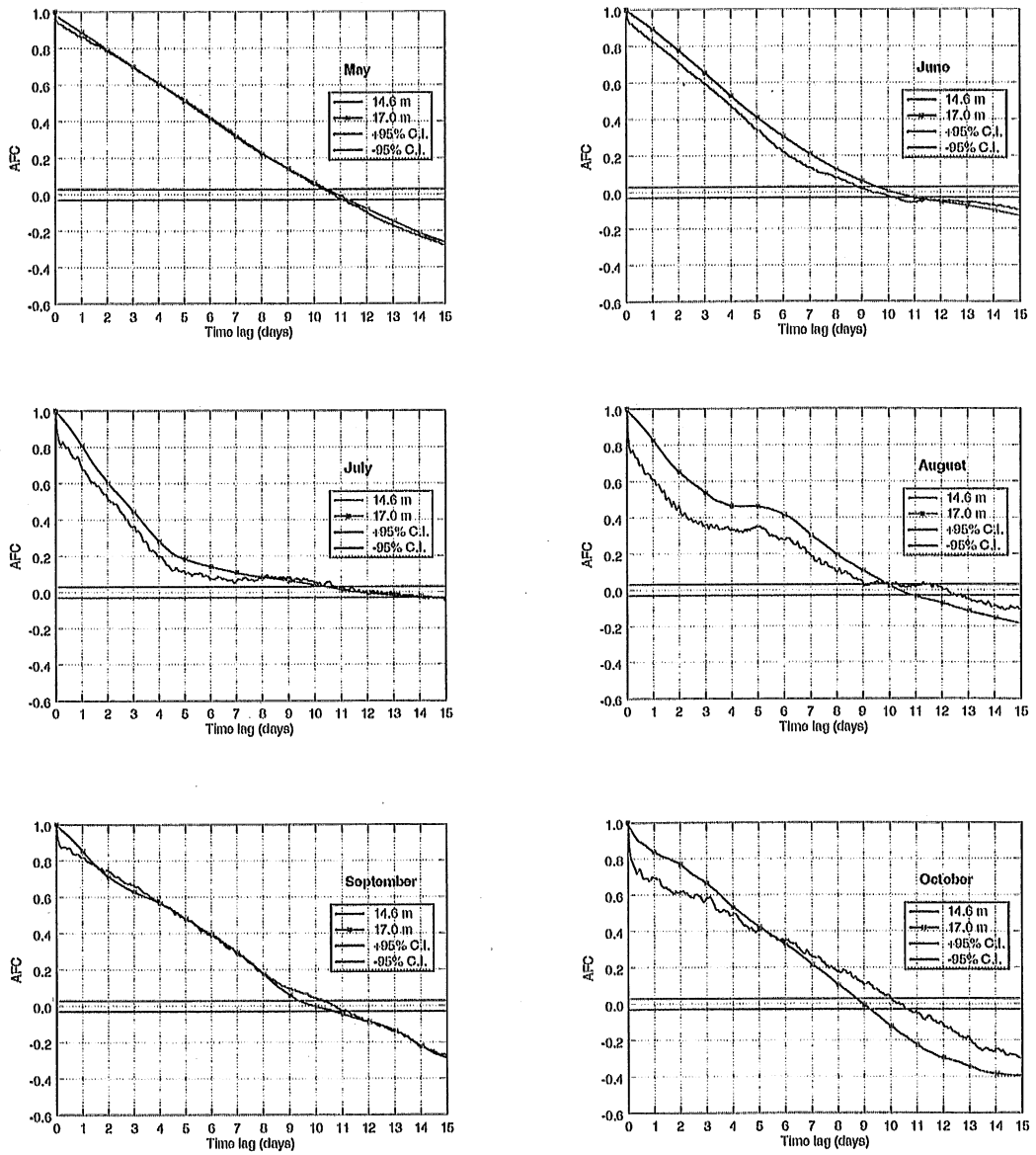

Figure 9: Autocorrelation coeffients of the temperature records for benthic layer (depths of 14.6 and 17.0 m) in the center of Lake McCarrons for the months of May to October, 1999.

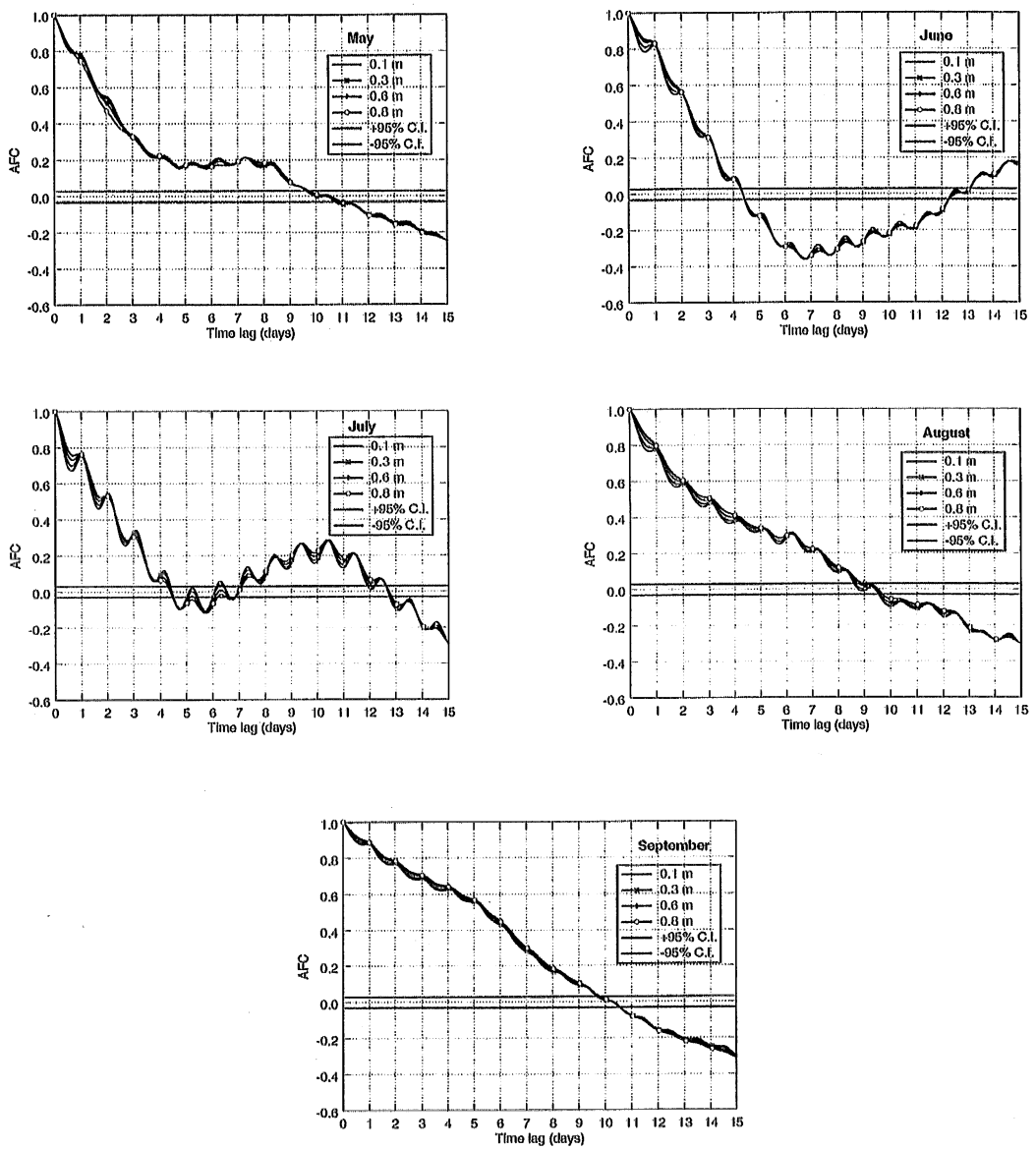

Figure 10: Autocorrelation coeffients of the temperature records for the surface layer (depths of 0.1, 0.3, 0.6, and 0.8 m) in the littoral region of Lake McCarrons for the months of May to September, 1999.

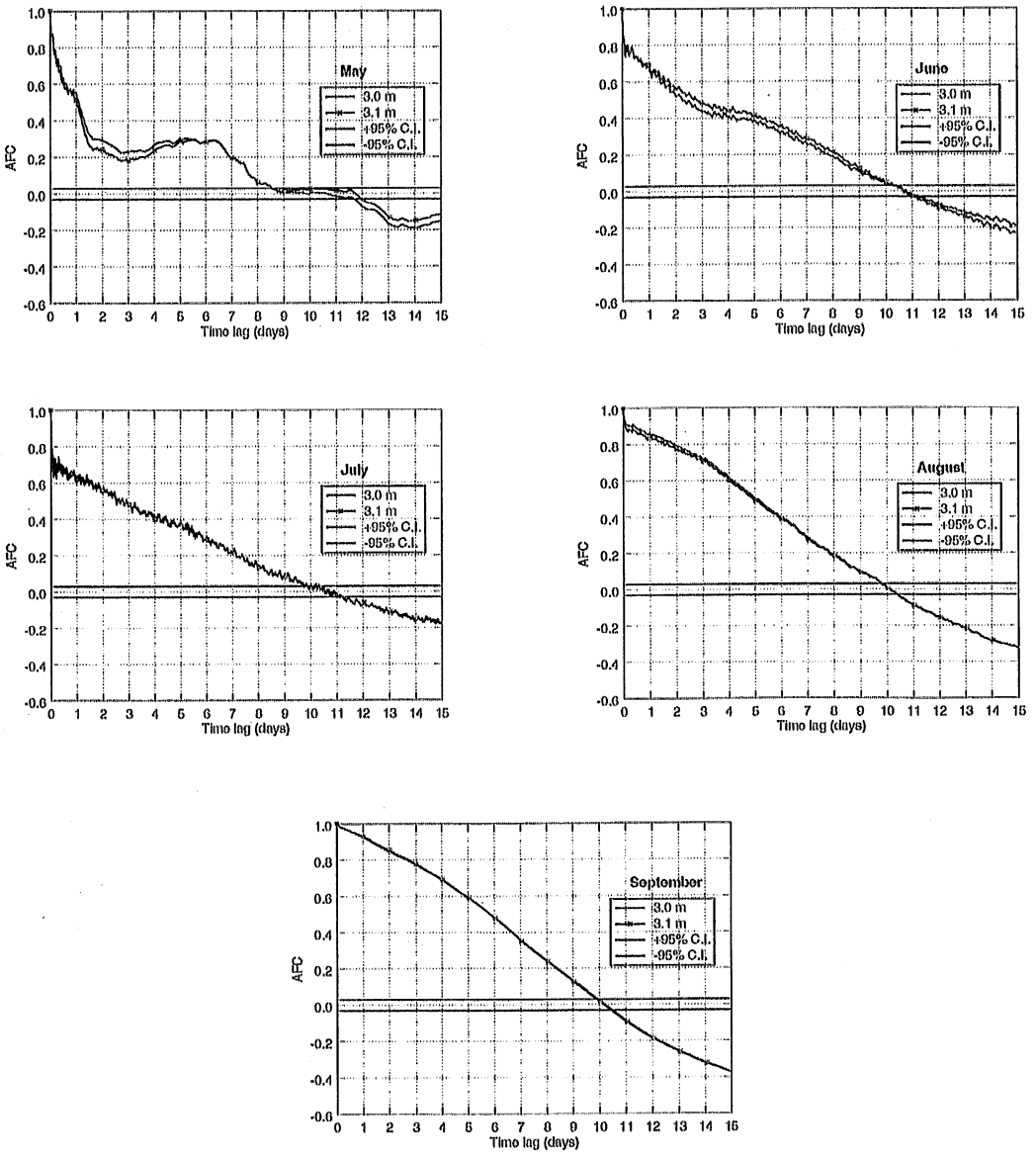

Figure 11: Autocorrelation coeffients of the temperature records for the benthic layer (depths of 3.0 and 3.1 m) in the littoral region of Lake McCarrons for the months of May to September, 1999.

Spring Overturn

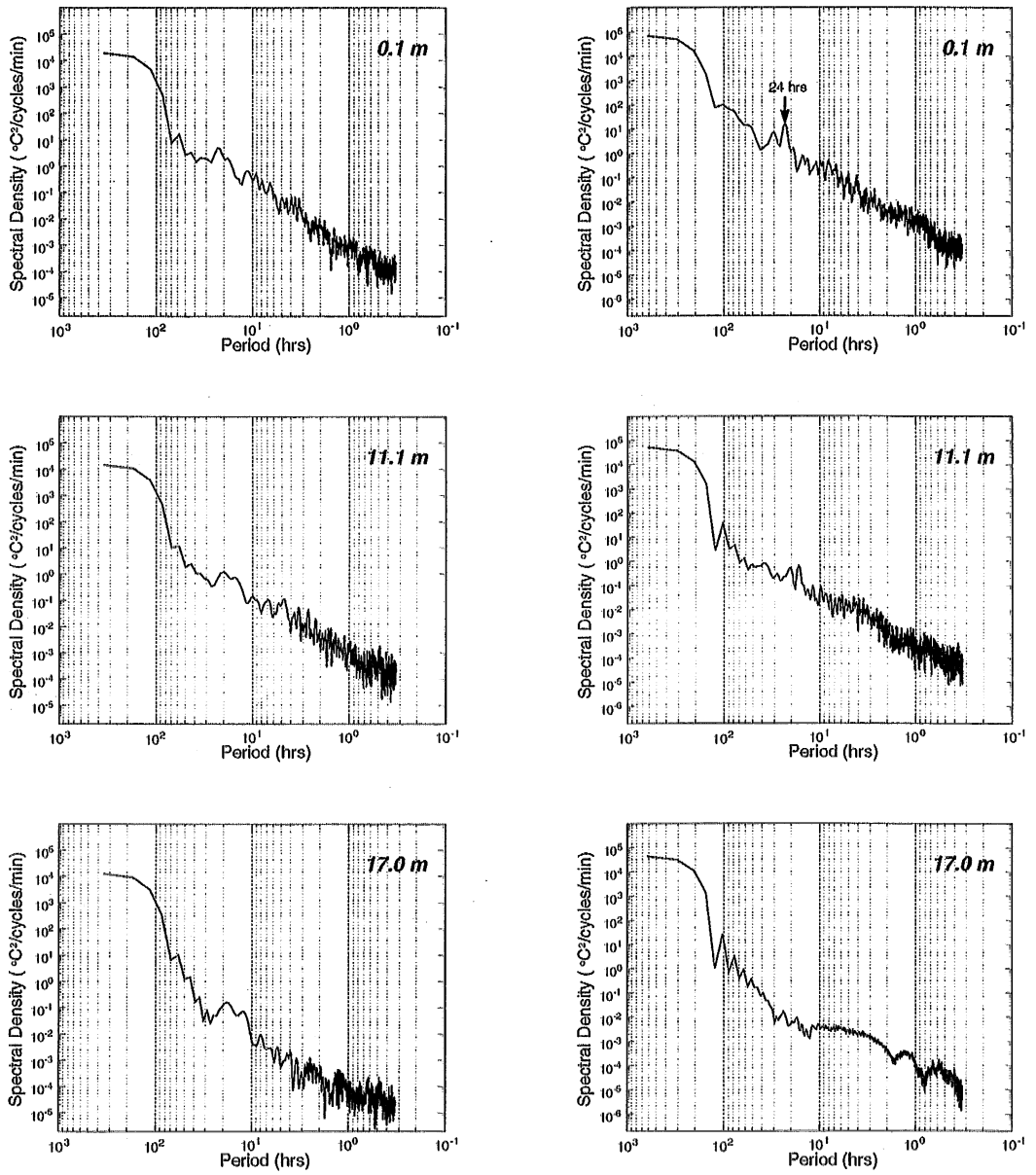

Figure 12: The surface mixed layer power spectra during Spring Overturn (March and April, 2000) at depth = 0.1 m, 11.1 m and 17.0 m (bottom). There is no stratification in March, and a weak stratification in April

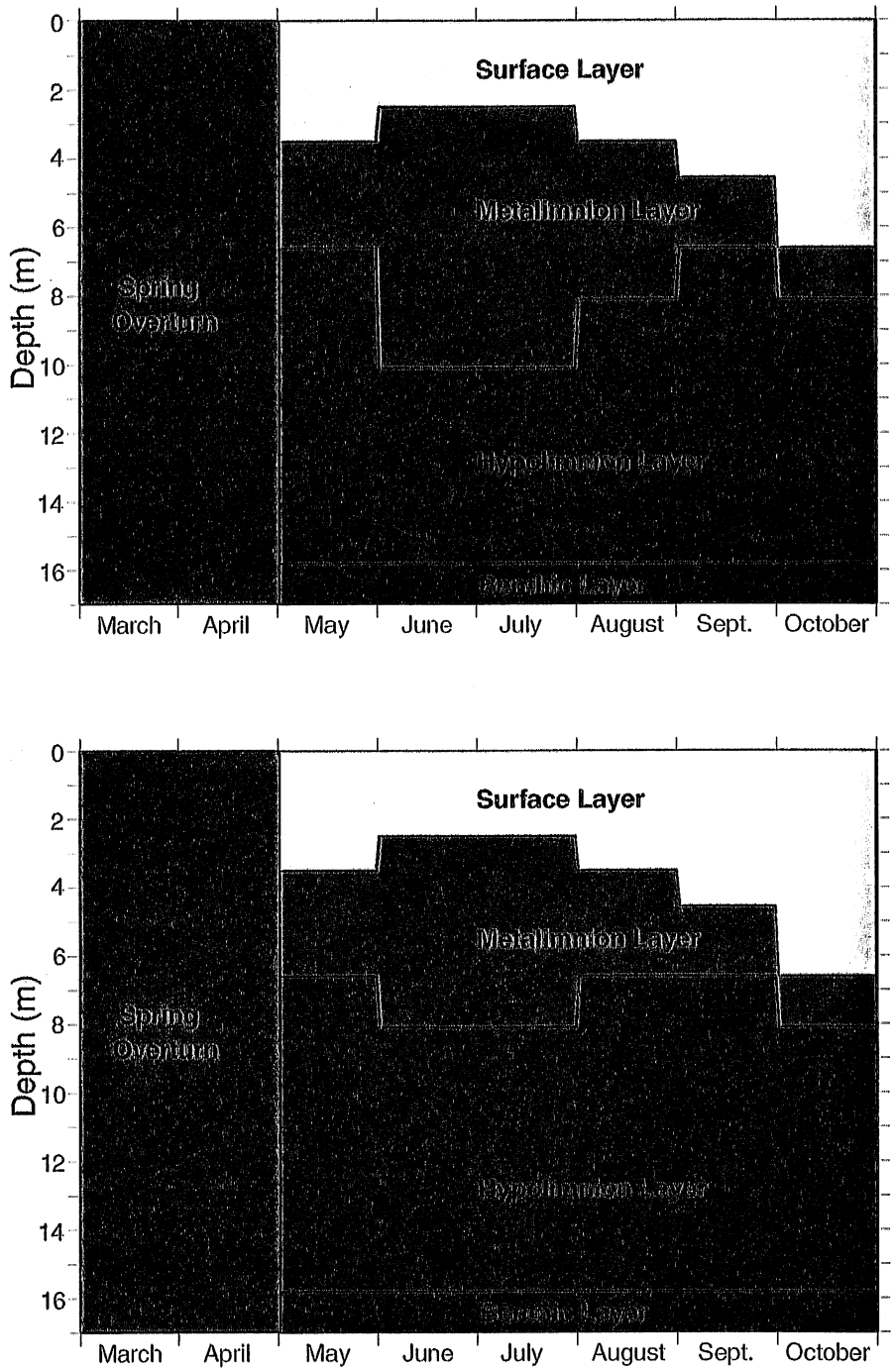

Figure 13: Depth and duration of characteristic layers (i.e. layers with similar stochastic water temperature signatures in the power spectral analysis) in the profundal region of Lake McCarrons, in 1999 (top) and 2000 (bottom).

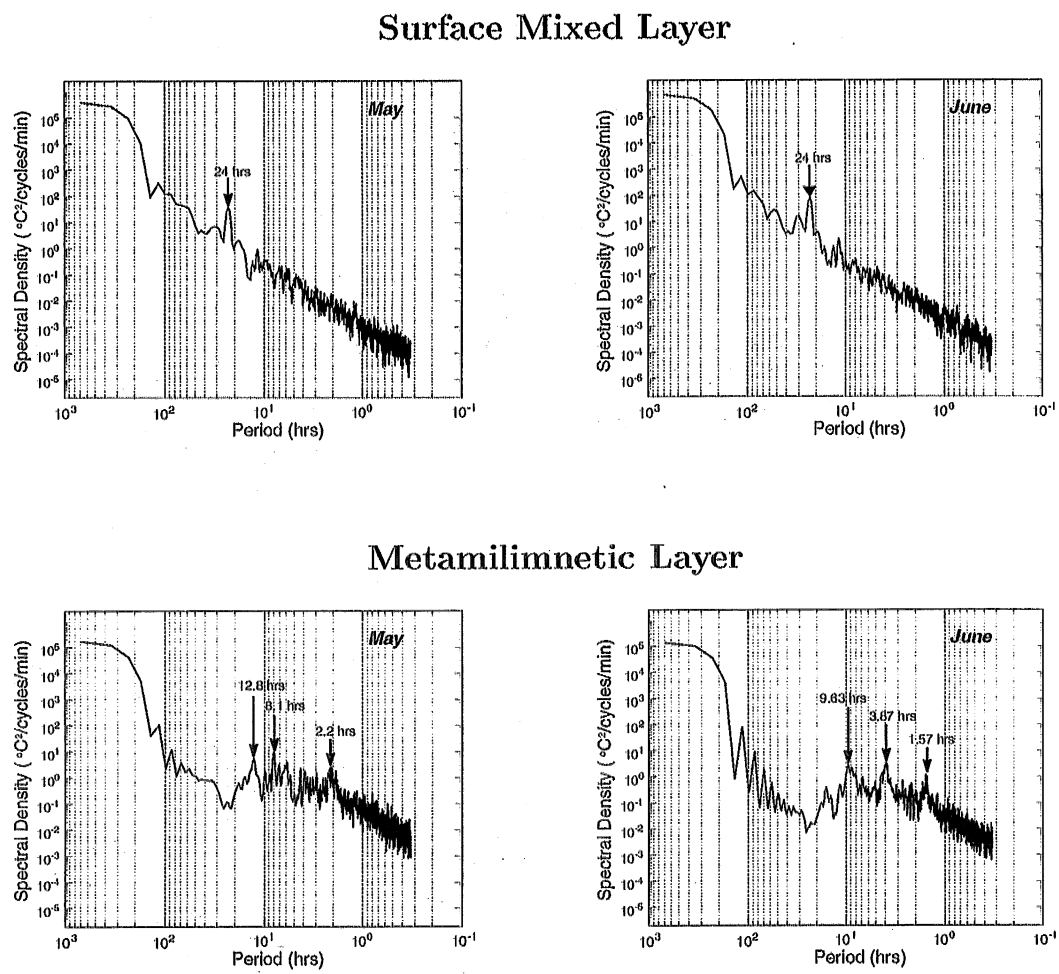

Figure 14: The surface mixed layer power spectra at depth = 0.1 m and the metamilimnion power spectra at depth = 6.1 m for May and June, 1999.

Hypolimnetic Layer

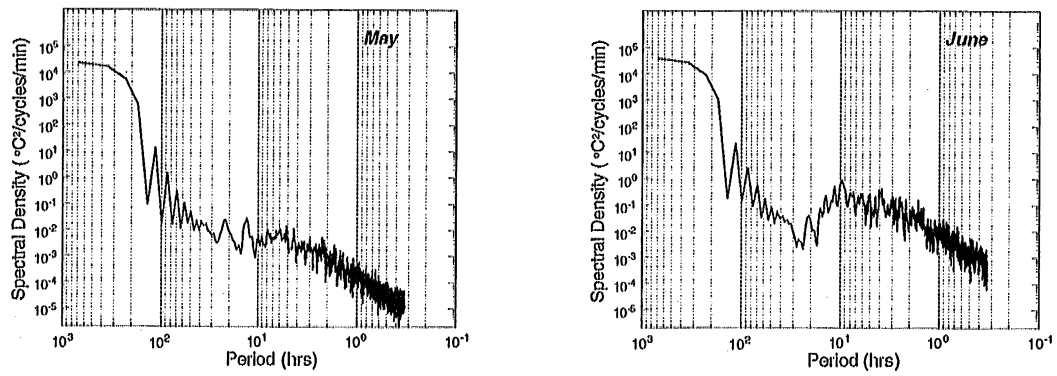

Benthic Layer

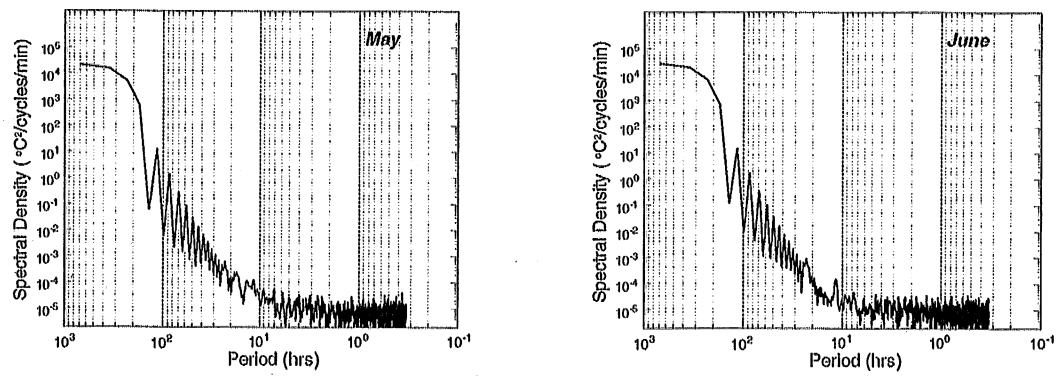

Figure 14: (cont'd) The hypolimnion power spectra at depth = 11.1 m and the benthic layer power spectra at depth = 17.0 m for May and June, 1999.

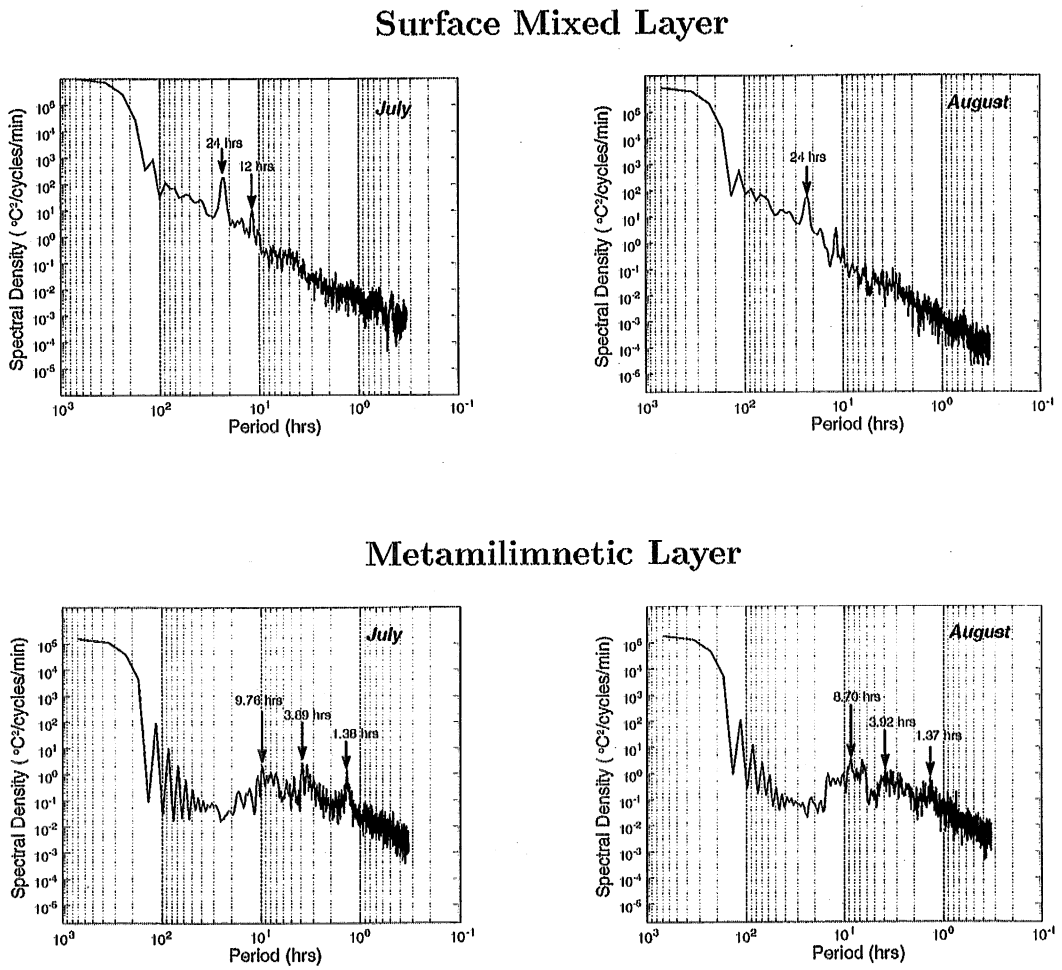

Figure 15: The surface mixed layer power spectra at depth = 0.1 m and the metamilimnion power spectra at depth = 6.1 m for July and August, 1999.

Hypolimnetic Layer

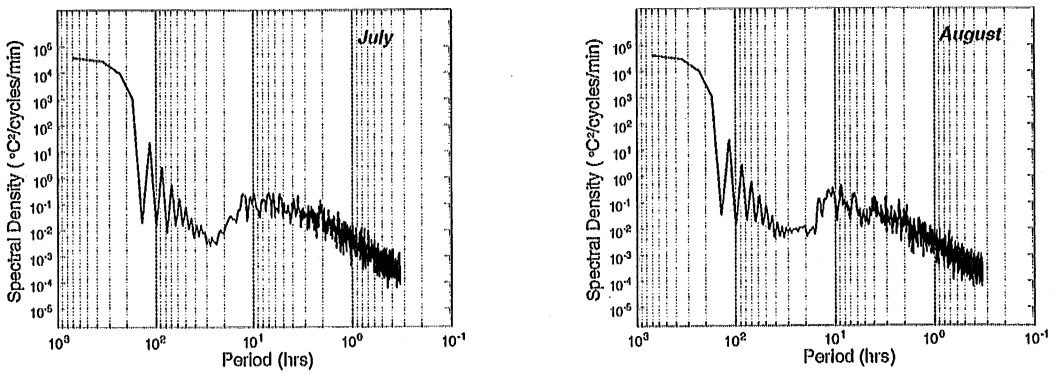

Benthic Layer

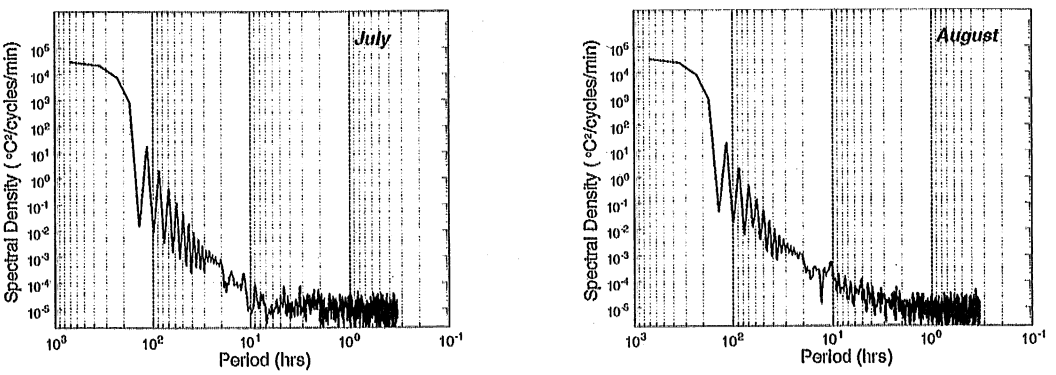

Figure 15: (cont'd) The hypolimnion power spectra at depth = 11.1 m and the benthic layer power spectra at depth = 17.0 m for July and August, 1999.

Surface Mixed Layer

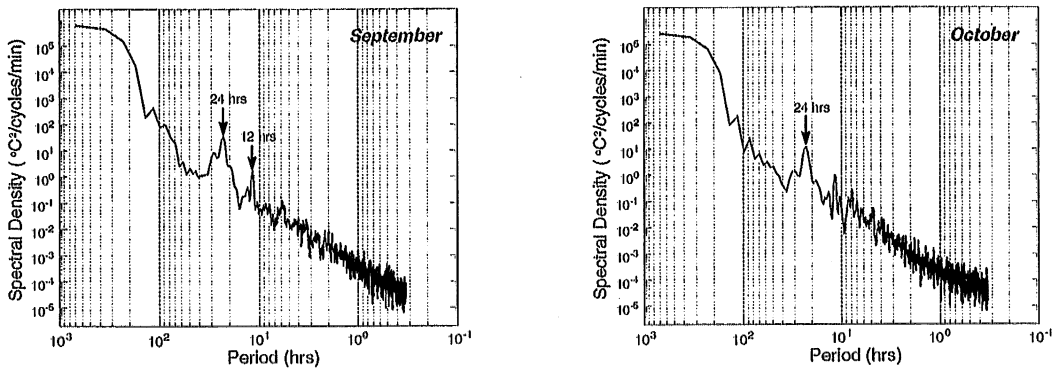

Metamilimnetic Layer

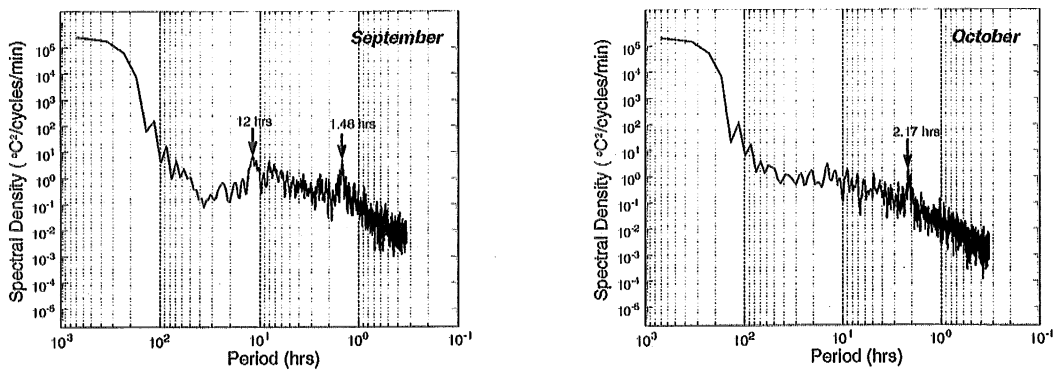

Figure 16: The surface mixed layer power spectra at depth = 0.1 m and the metamilimnion power spectra at depth = 6.1 m for September and October, 1999.

Hypolimnetic Layer

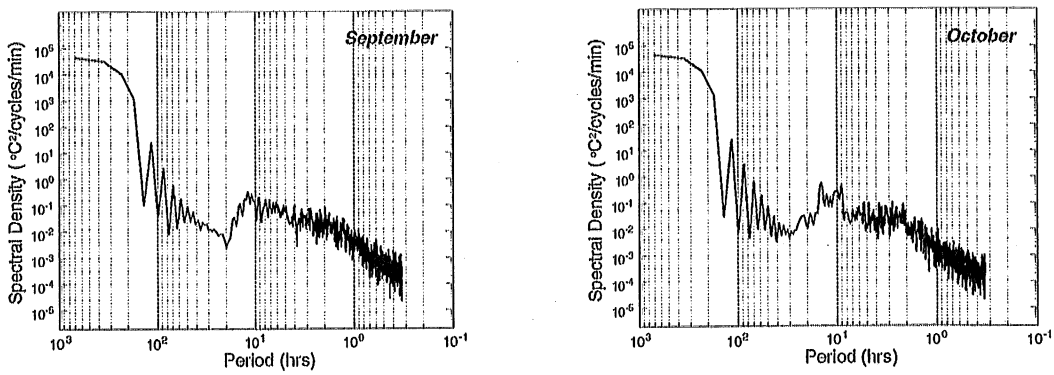

Benthic Layer

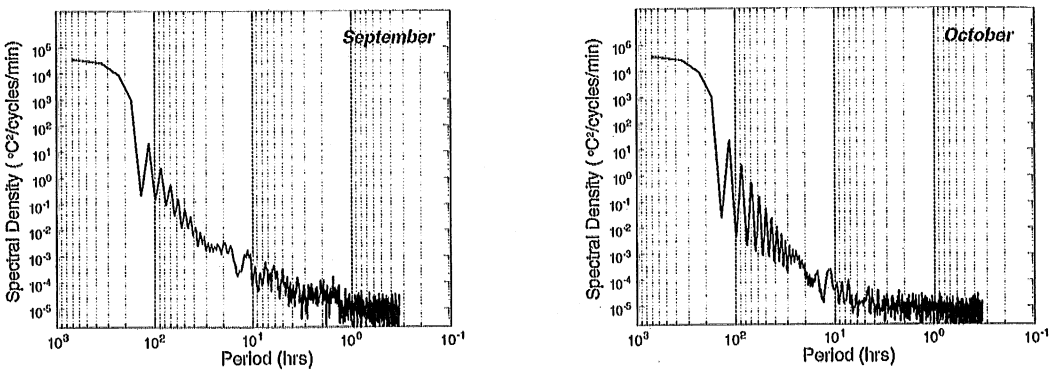

Figure 16: (cont'd) The hypolimnion power spectra at depth = 11.1 m and the benthic layer power spectra at depth = 17.0 m for September and October, 1999.

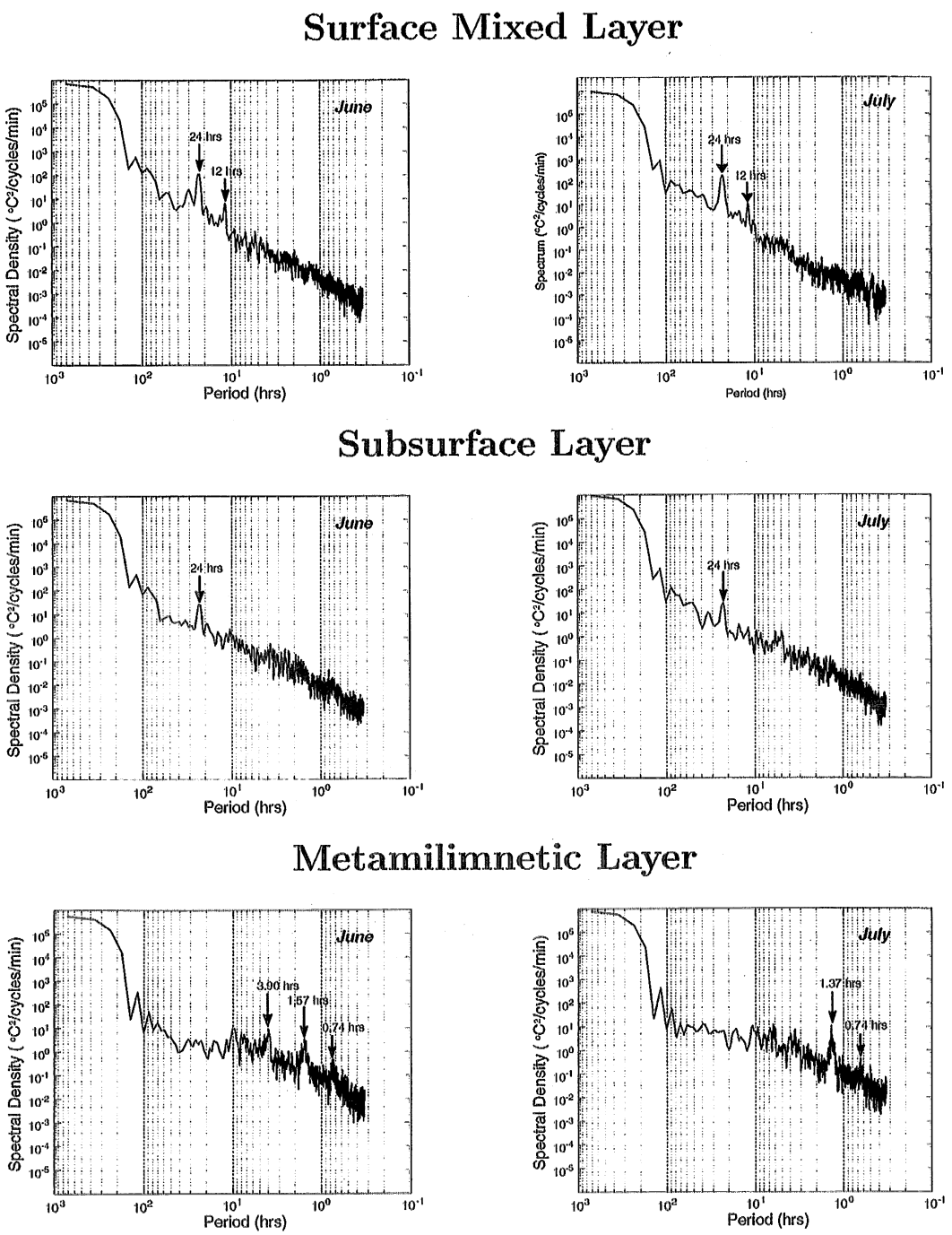

Figure 17: The power spectra in the surface mixed layer at depth = 0.1 m, in the subsurface layer at depth = 2.1 m, and in the benthic layer at depth = 3.0 m for the months of June and July 1999 in the littoral region of Lake McCarrons.

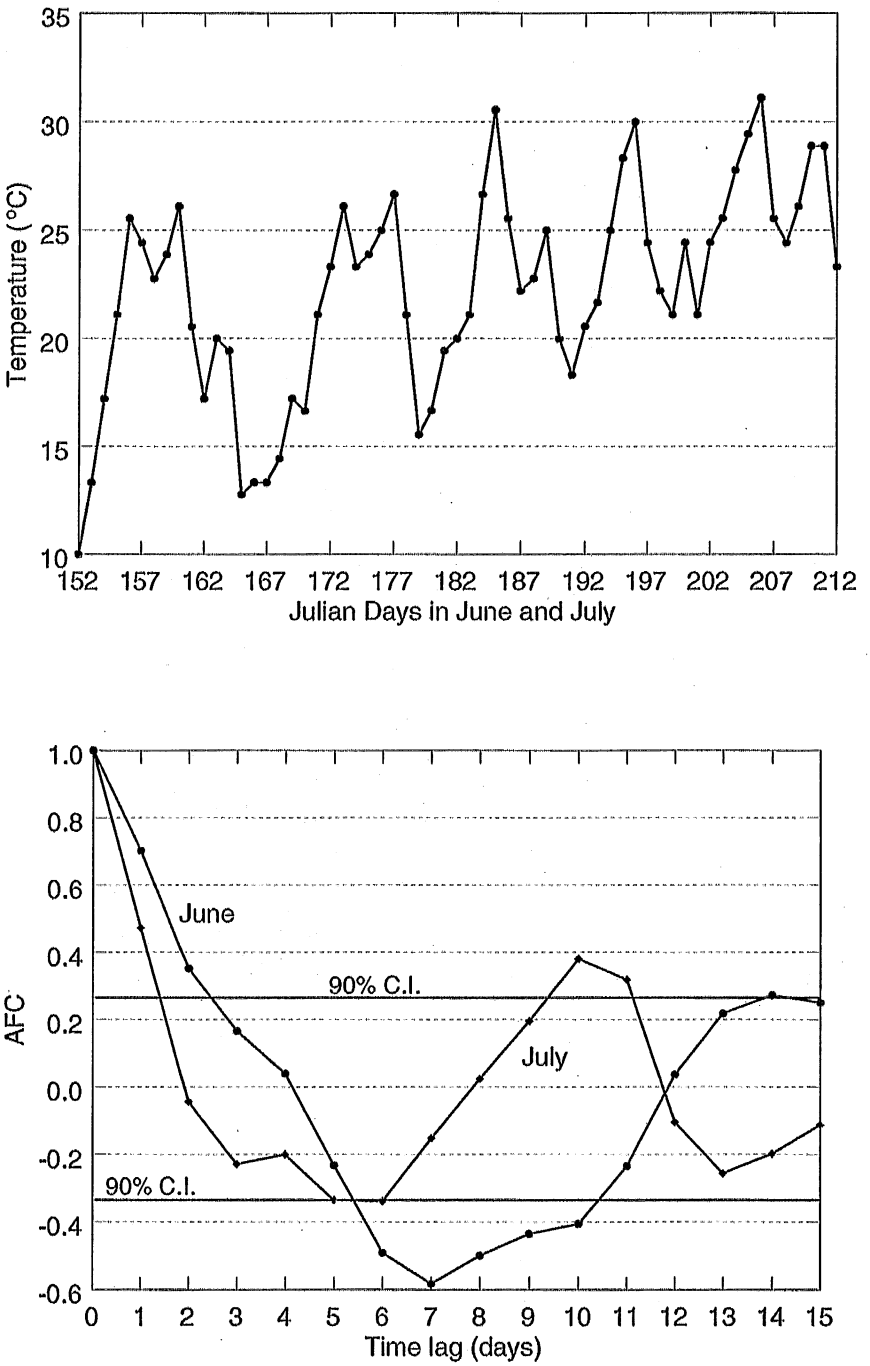

Figure 18: Air Temperature (top) and autocorrelation function (bottom) in the Twin Cities for the months of June and July, 1999.

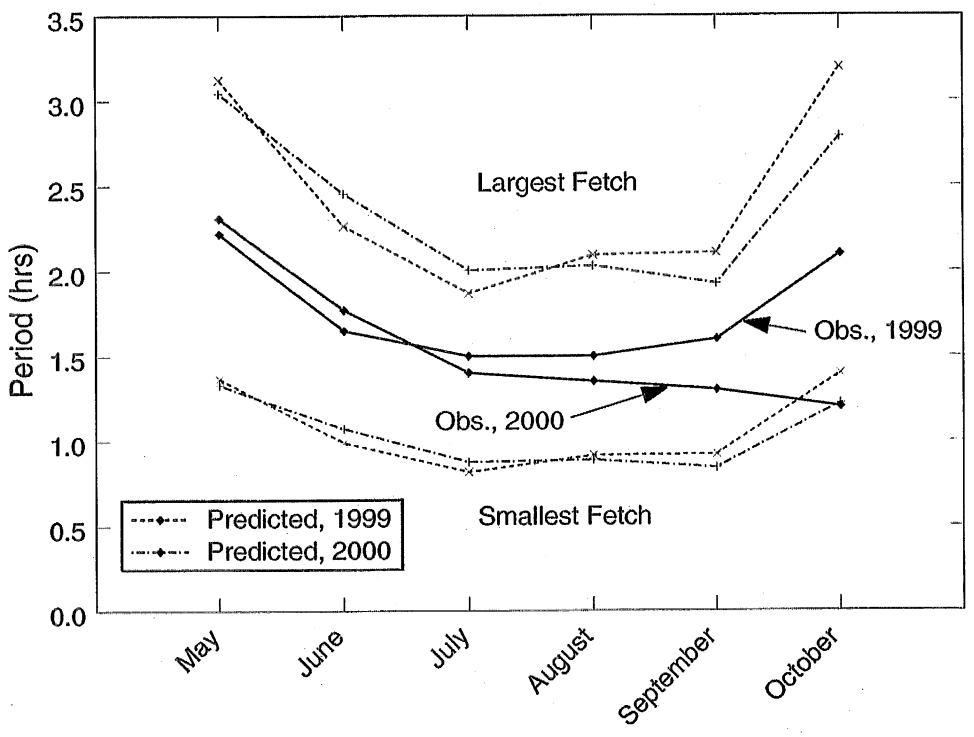

Figure 19: Predicted internal uninodal seiche periods and observed power spectral periods in the melalimnion at depth = 6.1 m. The largest fetch value at McCarrons Lake is 775.9 m and the smallest fetch is 339 m.